Dokkyo Journal of Medical Sciences
39(1) : 17～27, 2012

Original

NMDA Component of the Excitatory Synaptic Transmission of Neurons Containing Serotonin or GABA in the Ventrolateral Subdivision of the Periaqueductal Gray Matter of Mouse

Kenshu Shirakawa

Department of Anesthesiology, Dokkyo Medical University School of Medicine

SUMMARY

The midbrain periaqueductal gray (PAG) plays a crucial role in the descending pain modulating system. NMDA receptors (NMDARs) and serotonergic and GABAergic neurons have been identified in the PAG and are involved in the descending pain-modulating pathway. We characterized the NMDA component of the excitatory synaptic transmission within the ventrolateral subdivision of the PAG (vlPAG) using a whole cell patch clamp technique and then detected the expression of tryptophan hydroxylase (TPH), serotonin synthesizing enzyme, and glutamate decarboxylase (GAD), GABA synthesizing enzyme to understand the vlPAG intrinsic neurotransmission. The NMDA/non-NMDA ratio and the decay time constant of the NMDA component of the non-serotonergic GABAergic neurons were significantly larger than those of non-serotonergic non-GABAergic neurons and serotonergic GABAergic neurons. This suggests that the non-serotonergic GABAergic neurons might play an important role in the descending pain modulating system originated from the PAG. The decay time constant of the NMDA component of the non-serotonergic non-GABAergic neuron was significantly greater in the mouse with partial sciatic nerve ligation compared with the control mouse. These results suggest that the subunit composition of the NMDAR in the non-serotonergic non-GABAergic neurons change during neuropathic pain.

Key Words : Patch clamp recording, single-cell RT-PCR, sciatic nerve ligation, NMDA, PAG

INTRODUCTION

It is known that the midbrain periaqueductal gray (PAG) plays a crucial role in the descending pain modulating system. Many reports have demonstrated that electrical or chemical stimulation of the ventrolateral subdivision of the PAG (vlPAG) suppresses a number of nociceptive reflexes and results in profound analgesia[1~5].

GABAergic neurons have been identified in the PAG[6,7] and they play an important role in the descending pain control. Application of $GABA_A$ receptor antagonists, such as bicuculline or picrotoxin, evokes antinociception and can potentiate morphine-induced analgesia[8,9]. Serotonergic neurons have also been shown to be involved in the PAG. Clements et al.[10] revealed the presence of serotonin-like immunoreactive cell bodies located in the ventrolateral and ventromedial regions of the caudal PAG. Consistent evidence has shown that the antinociception elicited by the elec-

Received November 4, 2011 ; accepted December 1, 2011
Reprint requests to : Kenshu Shirakawa
Department of Anesthesiology, Dokkyo Medical University School of Medicine, Mibu, Tochigi 321-0293, Japan

trical stimulation of vlPAG is regulated by the serotonergic mechanism[11,12].

It has been suggested that NMDARs are involved in the nociceptive pathway including the PAG[13~15]. The intra-vlPAG infusions of NMDAR agonists provoke high-magnitude antinociception[16~18]. Electrophysiological investigation in the vlPAG neuron has revealed that excitatory synaptic transmission was mediated by glutamate acting on NMDA and non-NMDA receptors[19].

The aim of this report is to characterize the glutamatergic synaptic transmission in vlPAG neurons in reference to the expression of serotonin and GABA, and to find changes of those characteristics by neuropathic pain. Using control mice and mice with the partial ligation of sciatic nerve, we characterized the NMDA component of the excitatory synaptic transmission within the vlPAG, using a whole cell patch clamp technique and then classified the recorded neurons based on their expression of mRNA for tryptophan hydroxylase (TPH), serotonin-synthesizing enzyme, and glutamate decarboxylase (GAD), GABA-synthesizing enzyme, using single-cell reverse transcription-polymerase chain reaction (RT-PCR), to help gain insight into the vlPAG intrinsic neurotransmission.

METHODS

1. Animals

Adult male ICR mice (5-6 weeks old) were used in this experiment. The animals were kept at controlled room temperature under a 12-h/12-h light/dark cycle. The care and use of the animals were in accordance with the Dokkyo University Animal Care and Use Committee and the guidelines of the International Association for the Study of Pain[20].

2. Surgery

Mice were anesthetized by an intraperitoneal injection of sodium pentobarbital (50 mg/kg). The left sciatic nerve was partially ligated according to the protocol for rats as described by Seltzer et al.[21]. In sham-operated control mice, the sciatic nerve was exposed but not ligated.

3. Assessment of behavioral mechanics

Mice were placed on an elevated plastic mesh floor covered with a clear plastic box (height, 15 cm ; diameter, 12 cm) and the withdrawal threshold to mechanical stimulation was determined. The mechanical stimulus was applied from below the plantar aspect of the hind limb, ipsilateral to the partial nerve ligation by means of an Electro von Frey (Model 1601 ; IITC Inc., Woodland Hills, CA). The lowest force from five tests that induced a withdrawal response was considered the withdrawal threshold. The measurements were made from 2 days before the surgical operation through 10 days after the surgical operation.

4. Preparation of midbrain slices including PAG

Brain slices were made according to the methods described by Ye et al.[22]. Briefly, the mice were anesthetized with pentobarbital and decapitated. The brains were quickly removed and blocked. Transverse slices (350 μm) were cut by a vibratome through the entire rostro-caudal extent of the PAG. Slices were transferred to a recording chamber, which was continually superfused (2-3 ml/min) with an artificial cerebral spinal fluid of the following composition (in mM) : 124 NaCl, 3.2 KCl, 1.25 NaH_2PO_4, 26.0 $NaHCO_3$, 2.5 $CaCl_2$, and 1.3 $MgCl_2$ equilibrated with 95% O_2 − 5% CO_2. When necessary, $MgCl_2$ was not included to make a nominally Mg^{2+}-free solution.

5. Whole cell patch clamp recordings

Whole cell recordings were made from visually identified vlPAG cells of the brain slices. Patch pipettes were filled with an internal solution having the following ionic composition (mM) : potassium gluconate, 123 ; KCl, 14 ; sodium gluconate, 2 ; (ethylenebis (oxononitrilo)) tetraacetate, 1 ; HEPES, 10 ; pH neutralized to 7.4 with KOH. When making perforated patch clamp recordings, amphotericin B (6 μg/ml) was included in the pipette solution. The progress of perforation was monitored by measuring the access resistance deduced from the amplitude of the capacitive transients in response to repetitive 10mV hyperpolarizing steps. The DC resistance of the pipettes filled with the internal solution was 5-10 MΩ. All experiments were performed at room temperature.

Excitatory postsynaptic current (EPSC) was evoked at 0.1 Hz using a stimulating electrode filled with 1 M NaCl with its tip (diameter, ca.3 μm) placed about

200 μm away from the recording site. All recordings were made in the presence of strychnine (2.0 μM), bicuculline (10 μM). Non-NMDA component of the EPSC was recorded in the presence of APV (50 μM) at holding potential −70 mV. NMDA component of the EPSC was recorded in the presence of CNQX (30 μM) in the nominally Mg^{2+}-free solution at a holding potential of −70 mV. EPSCs were recorded in the voltage clamp mode using an Axopatch 200B patch clamp amplifier (Axon Instruments, USA). Data were sampled at a rate of 10.0 kHz through a Digidata 1230 interface (Axon Instruments). pCLAMP (Axon Instruments) was used to analyze the data.

6. Single-cell RT-PCR

After whole cell recordings were made, the neurons were aspirated into another pipette according to a previously described protocol[23]. The collecting pipette had a tip diameter of about 3-5 μm and contained 2 μl of Ca^{2+}- and Mg^{2+}-free phosphate-buffered saline solution. The neurons were then ejected into thin-walled autoclaved PCR tubes by applying a gentle positive pressure, and immediately frozen and stored at −80℃ until use. The PCR tubes contained 2 μl MgCl2 (25 mM), 2 μl 10 PCR buffer (200 mM Tris-HCl, 500 mM KCl), 0.5 μl RNase inhibitor (40,000 units/ml), 2 μl nonionic detergent IGEPAL CA-630 (5%), and 5 μl DEPC treated water.

On the following day, analysis was performed using IGEPAL CA-630 at room temperature for 5 min followed by the addition of the reverse transcription mixture. The RT mix contained 1 μl oligo (dT) primers (0.5 μg/μl), 2 μl mixed deoxynucleotide triphosphates (dNTPs, 10 mM), 2 μl dithiothreitol (0.1 M), 0.5 μl Rnase inhibitor (40,000 units/ml), and 1 μl SuperScript II RT (200 Units/μl). The reaction mixture was incubated at 42℃ for 50 min. Subsequently, the sample was heat-inactivated at 70℃ for 15 min.

The PCRs were performed using the protocol of Fukushima et al.[24] in a 50-μl volume containing 20 mM Tris-HCl, 50 mM KCl, 2.5 mM MgCl2, 0.2 mM dNTPs, and 2.5 units Taq DNA polymerase. The entire RT product was used for the first PCR, and 1-2 μl of the first PCR product was used for the second PCR. The primers were designed to target three genes, NSE, TPH, and GAD67. NSE was used as a positive control and we discarded the cells in which NSE RT-PCR product was absent. Primers used for detection of NSE were 5-ATAGTGGGCGATGACCTGAC-3 and 5-ATGAACGTGTCCTCCGTTTC-3 (200-bp product ; GenBank accession # NM 013509). Primers used for TPH detection were 5-TCCTTTGACCCAAAGACGAC-3 and 5-AGGTCCTGCACCACATTCTC-3 (215-bp product ; GenBank accession # NM 173391). Primers used for GAD67 detection were 5 -CAAGTTCTGGCTGATGTGGA-3 and 5-GCCACCCTGTGTAGCTTTTC-3 (231-bp product ; GenBank accession # NM 008077). These primers were used for both the first and second PCR amplification. Each primer was individually used in the second PCR. The concentration of primers was 20 nM each in the first PCR and 200 nM in the second PCR. The thermal cycler (Gene Amp 2400, Perkin Elmer) was programmed for 35-40 cycles of 1 min at 94℃ denaturation, 1 min at 54-59℃ for annealing, and 1 min at 72℃ for elongation. The second PCR products were visualized by staining with ethidium bromide and separated by agarose gel electrophoresis. All the products were sequenced using dye terminator chemistry (Applied Biosystems) and a DNA sequencer (Model 377, ABI) and matched the published sequences. All the reagents for the RT-PCR were obtained from GIBCO BRL, except the RNase inhibitor (TOYOBO), IGEPAL CA-630 (Sigma) and Taq DNA polymerase (Takara).

7. Statistical analysis

Results are expressed as mean ± SEM. Statistical analysis of the results was performed by un-paired t test for the analysis of effects of partial ligation of sciatic nerve on the characteristics of NMDA component and by 1way ANOVA with Dunnett's Multiple Comparison Test for the analysis of characteristics of the NMDA component of four phenotypes. Differences were considered significant at the level of $p < 0.05$.

RESULTS

1. Four phenotypes of neurons were distinguished by single cell RT-PCR

We collected individual neurons in the vlPAG after the recordings of synaptic current. The RNA from the neurons was extracted and processed for use in single-cell RT-PCR for NSE, TPH, and GAD67 to identify

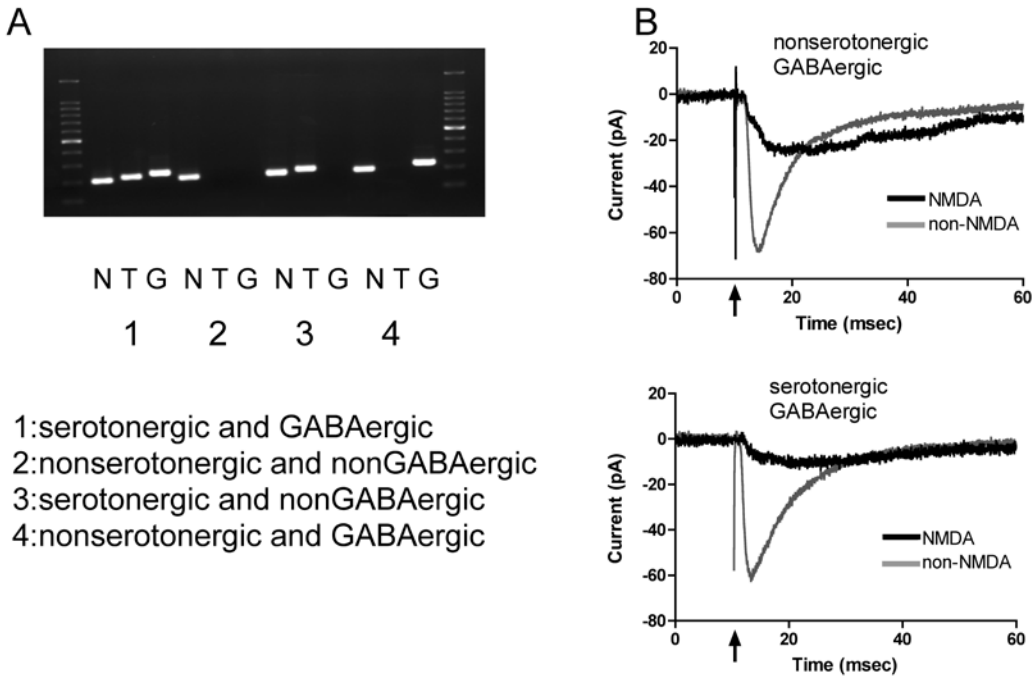

Figure 1 Examples of the RT-PCR and typical examples of recorded EPSC in the vlPAG. (**A**) Agarose gel analysis of the RT-PCR product of a single vlPAG neuron, expressing NSE (labeled with N), TPH (labeled with T), and GAD67 (labeled with G) transcripts. Based on the expression of TPH or GAD67, we identified four phenotypes, serotonergic GABAergic, serotonergic Non-GABAergic, non-serotonergic GABAergic, and non-serotonergic non-GABAergic neurons. (**B**) NMDA and non-NMDA component of EPSC were recorded using whole cell patch clamp technique. NMDA component of a typical example of synaptic current recorded in a non-serotonergic GABAergic neuron (upper trace) was larger than that recorded in a serotonergic GABAergic neuron (lower trace). Electrical stimulation was applied at the time indicated by an arrow.

the gene expression of the neuron-specific enolase, serotonin-synthesizing enzyme, and GABA-synthesizing enzyme. Examples of RT-PCR data are shown in Figure 1A. Presence of TPH RT-PCR product served as an indicator of the presence of serotonin in the neuron. The presence of DAD67 RT-PCR product served an indication that the neuron contained GABA. Of the 79 NSE-positive cells, 48 expressed THP (61%) (serotonergic) and 51 expressed GAD67 (65%) (GABAergic). Co-expression of these markers was found in 35 neurons (44%). Therefore, four phenotypes of neurons were distinguished (Fig. 1A), neurons containing serotonin and GABA (named as serotonergic GABAergic neuron) (n=35, 44%), neurons containing serotonin but not GABA (named as serotonergic non-GABAergic neuron) (n=13, 17%), neurons containing GABA but not serotonin (named as non-serotonergic GABAergic) (n=16, 20%), and neurons containing neither serotonin nor GABA (named as non-serotonergic non-GABAergic) (n=15, 19%). Our next step was to test whether the four different phenotypes were different in their synaptic functions.

2. NMDA and non-NMDA components of the vlPAG neurons

Excitatory postsynaptic current (EPSC) was recorded using a stimulating electrode placed about 200 μm away from the recording site. The NMDA and non-NMDA components of the EPSC were pharmacologically distinguished. Relative magnitude and decay kinetics of NMDA component of the EPSCs were examined. Typical examples of NMDA and non-NMDA components are shown in Figure 1B. The ratio of the peak value of NMDA component to that of non-NMDA component (NMDA/non-NMDA ratio) of the non-serotonergic GABAergic neuron was larger than that of the serotonergic GABAergic neuron (Fig. 1B).

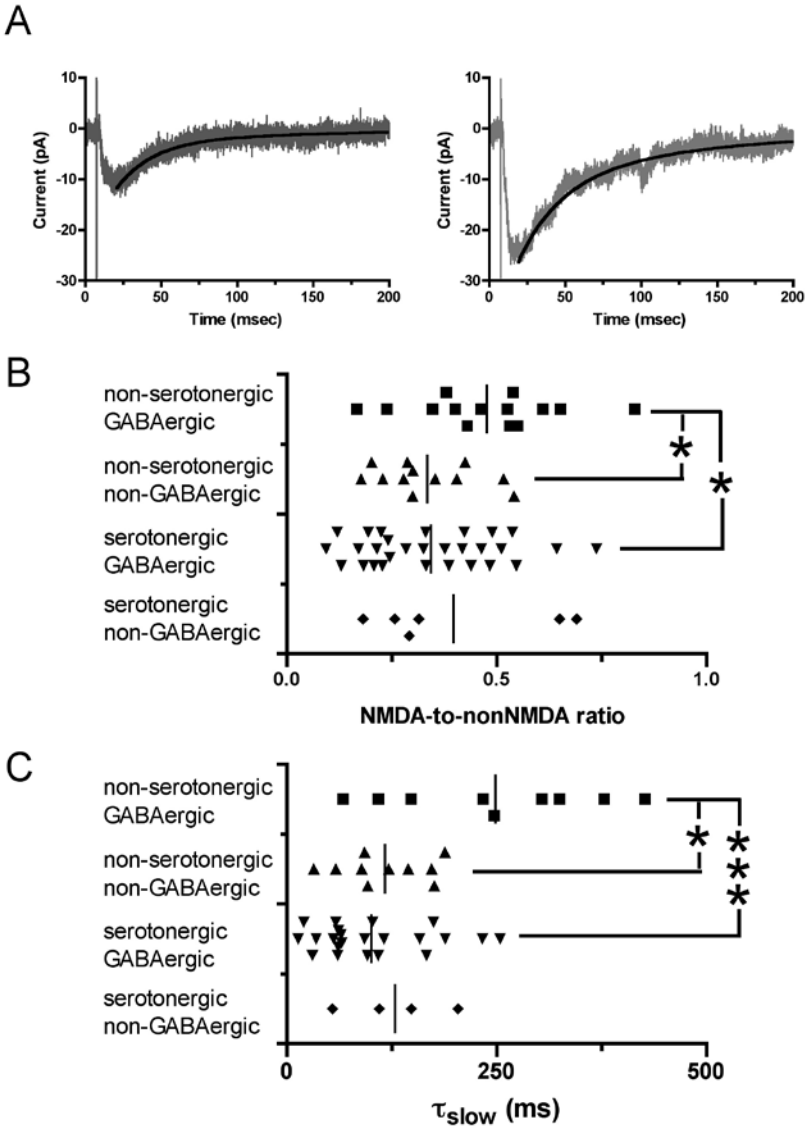

Figure 2 Characteristics of the NMDA component of four phenotypes in the vlPAG. (**A**) The decay of NMDA EPSC was fit with a biexponential function having a fast (τ_{fast}) and a slow (τ_{slow}) decay time constant. Superimposed biexponential function fits well with the decay phase of the NMDA component. Two typical examples with different phenotypes were shown. (**B**) Ratio of NMDA component to non-NMDA component of EPSC in the four different phenotypes. The NMDA/non-NMDA ratio of the non-serotonergic GABAergic neurons was larger than those of other neuron types. The differences are significant when being compared with the non-serotonergic non-GABAergic neurons and the serotonergic GABAergic neurons. (**C**) Decay time constant of NMDA component. The value of τ_{slow} of the NMDA component in the non-serotonergic GABAergic neurons was larger than those of the other neuron types. The differences are significant when being compared with that of non-serotonergic non-GABAergic neurons and the serotonergic GABAergic neurons. Vertical lines within each graph indicate mean values. $^{*}P<0.05$, $^{***}P<0.005$.

3. NMDA/non-NMDA ratio of the non-serotonergic GABAergic neurons is significantly larger

Mean values of NMDA/non-NMDA ratios in the four different phenotypes of neurons were as follows ; 0.476±0.0454 (n=14) in the non-serotonergic GABAergic neurons, 0.335±0.0338 (n=12) in the non-serotonergic non-GABAergic neurons, 0.344±0.0305 (n=29) in the serotonergic GABAergic neurons, and 0.398±0.0883 (n=6) in the serotonergic non-GABAergic neurons. The NMDA/non-NMDA ra-

tio in the non-serotonergic GABAergic neurons was larger than those of other phenotypes (Fig. 2B). The differences are significant when being compared with those of non-serotonergic non-GABAergic neurons and serotonergic GABAergic neurons.

4. Decay time constant of the NMDA component in the non-serotonergic GABAergic neurons was significantly larger

We next examined the decay kinetics of NMDA component in the different neuron types. The decay phase of the NMDA component was fit with a biexponential function having a fast (τ_{fast}) and a slow (τ_{slow}) decay time (Fig. 2A, superimposed curves). The corresponding mean values of τ_{fast} and τ_{slow} of the four different types of neurons were as follows ; 27.47±11.42, 248.7±40.88 (n=9) in the non-serotonergic GABAergic neurons, 26.29±10.94, 117.0±16.59 (n=10) in the non-serotonergic non-GABAergic neurons, 14.32±3.928, 100.7±14.48 (n=22) in the serotonergic GABAergic neurons, and 25.43±15.03, 129.0±31.49 (n=4) in the serotonergic non-GABAergic neurons. The values of τ_{fast} of the four phenotypes were not significantly different from each other. However, the value of τ_{slow} of the NMDA component in the non-serotonergic GABAergic neurons was larger than other phenotypes (Fig. 2C). The differences are significant when being compared with those of non-serotonergic non-GABAergic neurons and serotonergic GABAergic neurons.

5. Neuronal phenotypes of the mouse with sciatic nerve partial ligation

In the next step, we used mice that had received partial ligation of the sciatic nerve. We collected individual neurons in the vlPAG of the mice with partial sciatic nerve ligation after the recordings of synaptic current. The extracted RNA was processed for examining the expression of NSE, TPH, and GAD67 using single-cell RT-PCR. Of the 61 NSE-positive cells, 24 neurons expressed THP (39%) (serotonergic), whereas 47 neurons expressed GAD67 (77%) (GABAergic). Co-expression of these markers was found in 22 neurons (36%). Therefore, four phenotypes of neurons were identified : serotonergic GABAergic (n=22, 36%), serotonergic non-GABAergic (n=2, 3%), non-serotonergic GABAergic (n=25, 41%), and non-serotonergic non-GABAergic (n=12, 20%). In comparison to the control mouse, the percentage of the serotonergic non-GABAergic neurons decreased significantly, and that of the non-serotonergic GABAergic neurons increased significantly in the mouse with partial sciatic nerve ligation. In the next step, the effects of ligation on the relative magnitude and decay kinetics of NMDA component of the EPSCs were examined.

6. The NMDA/non-NMDA ratio of non-serotonergic non-GABAergic neurons was significantly greater in the mouse with partial ligation

Mean values of NMDA/non-NMDA ratios in the four different phenotypes were as follows : 0.440±0.0392 (n=22) in the non-serotonergic GABAergic neurons, 0.459±0.0354 (n=12) in the non-serotonergic non-GABAergic neurons, 0.401±0.0548 (n=16) in the serotonergic GABAergic neurons, and 0.569±0.00294 (n=2) in the serotonergic non-GABAergic neurons. The NMDA/non-NMDA ratio of non-serotonergic non-GABAergic neuron was significantly greater in the mouse with partial ligation than in the control mouse (Fig. 3A). The ratios of the other neuron types were not significantly different between the control mouse and the mouse with nerve ligation.

7. Decay time constant of NMDA component of the non-serotonergic non-GABAergic neuron was significantly greater in the mouse with partial ligation

We examined the effect of nerve ligation on the decay kinetics of NMDA component. The mean values of τ_{slow} of the four different phenotypes were as follows : 139.8±39.51 (n=12) in the non-serotonergic GABAergic neurons, 571.7±180.8 (n=8) in the non-serotonergic non-GABAergic neurons, 179.4±98.61 (n=10) in the serotonergic GABAergic neurons, and 68.92±0.0 (n=1) in the serotonergic non-GABAergic neurons. The value of τ_{slow} of the NMDA component in the non-serotonergic GABAergic neurons was significantly larger than those of the non-serotonergic non-GABAergic neurons and the serotonergic GABAergic neurons. The value of τ_{slow} of the non-serotonergic GABAergic neuron was significantly smaller in the control mouse than in the ligation mouse. On the other hand, the value of τ_{slow} of the non-serotonergic non-

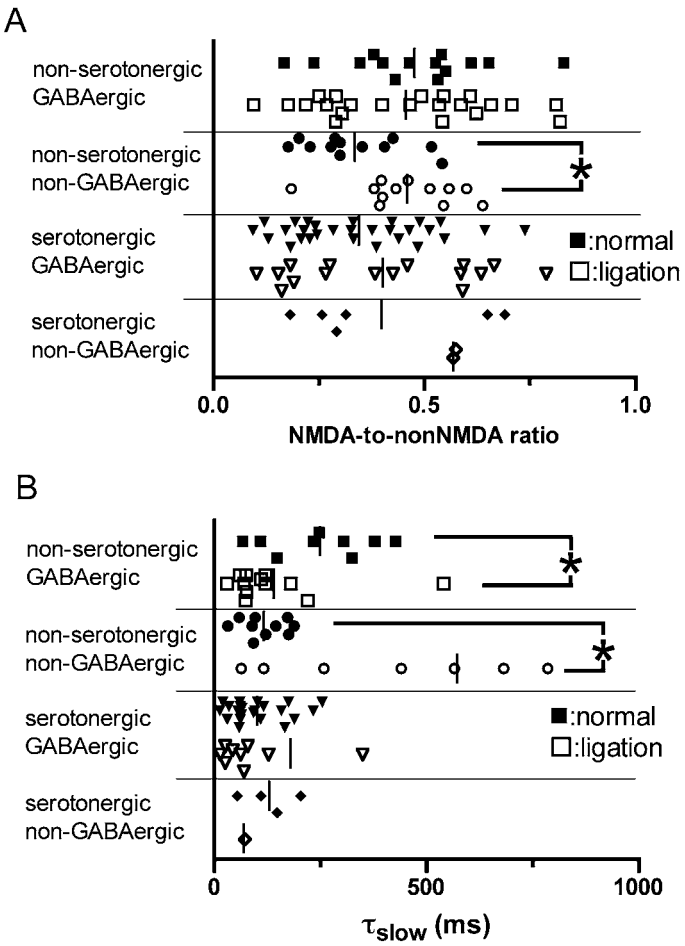

Figure 3 Effects of partial ligation of sciatic nerve on the characteristics of NMDA component of four phenotypes in the vlPAG. (**A**) Effects of ligation on the NMDA/non-NMDA ratio in the four different phenotypes. The ratio of non-serotonergic non-GABAergic neuron was significantly greater in the mouse with partial sciatic nerve ligation than in the control mouse. (**B**) Effects of ligation on the decay time constant of NMDA component. The value of τ_{slow} of the non-serotonergic non-GABAergic neuron was significantly greater in the mouse with partial sciatic nerve ligation than in the control mouse. Vertical lines within each graph indicate mean values. $^{*}P<0.05$, $^{***}P<0.005$.

GABAergic neuron was significantly greater in the mouse with partial ligation than in control mouse (Fig. 3B). The values of τ_{slow} of the other neuron types and the values of τ_{fast} of four phenotypes were not significantly different between the control mouse and the mouse with nerve ligation.

DISCUSSION

1. Slow decay time constant of NMDA component in the non-serotonergic GABAergic neurons

The decay time constant of the NMDA component and the NMDA/non-NMDA ratio of the non-serotonergic GABAergic neurons was larger than those of other neuronal phenotypes. Therefore, larger and longer depolarization would be elicited in the non-serotonergic GABAergic neurons than in other neuron types in response to synaptic inputs. PAG receives nociceptive ascending inputs originating from the spinal cord[25,26] and projects to spinal cord via the rostral ventromedial medulla (RVM) to modulate nociceptive transmission in the spinal cord[27,28]. Therefore, we postulate that the non-serotonergic GABAergic neurons might play an important role in the descending pain

modulating system originating from PAG.

2. Slow decay time constant of NMDA component in the non-serotonergic GABAergic neurons might come from the NMDA subunit composition

The difference in kinetics of the NMDA component between the non-serotonergic GABAergic neurons and the other phenotypes might reflect the difference in the subunit composition of NMDAR. NMDARs are multimeric proteins that are composed of NR1 subunits along with subunits of the NR2 family (NR2A-D)[29,30]. Combination of molecular biology and electrophysiological techniques have been used to show that expression of different glutamate receptor subunits underlies the alteration of the functional properties of NMDARs, including the time course of EPSCs in neurons[31~33]. The decay time constant of NR2A subunit was shorter than the other subunit NR2B-D. Based on the value of the recorded decay time constant of the non-serotonergic GABAergic neuron, 248.7±40.88 msec, we expect the non-serotonergic GABAergic neurons to be composed of more NR2B or C subunits and less NR2A subunits than other neuron type.

3. Characteristics of NMDA component of the non-serotonergic non-GABAergic neuron changed after partial ligation of sciatic nerve

In the neurons of the spinal cord, the functional properties of the NMDAR change during neuropathic pain induced by peripheral nerve injury[34,35]. Iwata et al.[36] showed that after partial ligation of the sciatic nerve, decay time constant of the NMDA component of the spinal cord neurons was increased and expression of NR2B subunit was increased. This suggests that the subunit composition of the sub-synaptic NMDARs in the superficial dorsal horn was altered by peripheral nerve injury. We found that the time constant of NMDA component of the non-serotonergic non-GABAergic neuron in the vlPAG was significantly greater in the mouse with partial sciatic nerve ligation than in the control mouse. The decay time constant NMDAR could vary depending on subunit composition. The NR2A subunit is shorter, NR2B and C are longer, and NR2D is much longer. Therefore we speculate that a change of subunit composition underlies the increase in the decay time constant in the vlPAG neurons after the partial ligation of the sciatic nerve.

4. Single cell RT-PCR analysis of GAD67 and TPH expressed in the vlPAG

We found a significant decrease in the percentage of the serotonergic non-GABAergic neurons and significant increase in the percentage of the non-serotonergic GABAergic neurons after partial sciatic nerve ligation. A previous report showed that chronic pain induced by nerve injury elicited temporal changes in mRNA expression for substance P, dymorphin, and enkephalin in the spinal cord[37]. Abraham et al.[38] also observed an increase in mRNA expression of opioids in spinal and supraspinal levels following spinal cord injury. Therefore, we propose that the change of in the mRNA expression for TPH and GAD67 in the vlPAG neurons occurred during neuropathic pain.

Serotonergic neurons in the PAG project to RVM[39]. RVM directly projects to the spinal cord and modulates the nociceptive transmission[27,28]. Majority of the GABAergic neurons are interneurons[6,40] and tonically inhibit the projection neurons in the PAG[9,41]. There has been a hypothesis that disinhibition due to a decrease in tonic inhibition leads to the antinociceptive effect. Taking this hypothesis into consideration, the increase in the non-serotonergic GABAergic neurons and the decrease in the serotonergic non-GABAergic neurons lead to the decrease in antinociception that is elicited during neuropathic pain. One possible explanation is that these phenotype changes might be related to a mechanism other than antinociception in the pain modulating system, for example, the hyperalgesia[42,43] elicited after nerve injury.

Another explanation for the phenotype change is that the serotonergic non-GABAergic neurons might be related to stress-induced sympathetic activity. The subpopulation of serotonergic projections from the vlPAG was shown to be capable of inhibiting stress-induced sympathetic activity in the region of the C1 A neurons in the RVM[44]. The C1 A neurons are important sympathoexcitatory neurons that initiate pressor responses in the presence of stressful stimuli[45]. We speculate that the significant decrease in the percentage of the serotonergic non-GABAergic neurons could be related to the modulation of the sympathoexcitatory response elicited by chronic pain.

5. Conclusion

We compared the NMDA/non-NMDA ratio and the decay time constant of the NMDA component of the synaptic current between four different neuronal phenotypes detected by single-cell RT-PCR based on the expression of TPH and GAD67. The NMDA/non-NMDA ratio and the decay time constant of the NMDA component of the non-serotonergic GABAergic neurons were significantly larger than that of non-serotonergic non-GABAergic neurons and the serotonergic GABAergic neurons. We also found that the decay time constant of NMDA component of the non-serotonergic non-GABAergic neuron were significantly greater in the mouse with sciatic nerve partial ligation than in the control mouse. These results suggest that the non-serotonergic GABAergic neurons might play an important role in the descending pain modulating system originating from the PAG, and that the subunit composition of the NMDAR in the non-serotonergic non-GABAergic neurons change during neuropathic pain.

REFERENCES

1) Giesler GJ and Liebeskind JC : Inhibition of visceral pain by electrical-stimulation of periaqueductal gray-matter. Pain **2** : 43-48, 1976.
2) Morgan MM, Gold MS, Liebeskind JC, et al : Periaqueductal gray stimulation produces a spinally mediated, opioid antinociception for the inflamed hindpaw of the rat. Brain Res **545** : 17-23, 1991.
3) Lin Q, Peng YB, Willis WD : Glycine and gaba (a) antagonists reduce the inhibition of primate spinothalamic tract neurons produced by stimulation in periaqueductal gray. Brain Res **654** : 286-302, 1994.
4) Waters AJ and Lumb BM : Inhibitory effects evoked from both the lateral and ventrolateral periaqueductal grey are selective for the nociceptive responses of rat dorsal horn neurones. Brain Res **752** : 239-249, 1997.
5) Manning BH and Franklin KBJ : Morphine analgesia in the formalin test : Reversal by microinjection of quaternary naloxone into the posterior hypothalamic area or periaqueductal gray. Behav Brain Res **92** : 97-102, 1998.
6) Barbaresi P and Manfrini E : Glutamate decarboxylase-immunoreactive neurons and terminals in the periaqueductal gray of the rat. Neuroscience **27** : 183-191, 1998.
7) Barbaresi P : GABA-immunoreactive neurons and terminals in the cat periaqueductal gray matter : A light and electron microscopic study. J Neurocytol **34** : 471-487, 2005.
8) Moreau JL and Fields HL : Evidence for gaba involvement in midbrain control of medullary neurons that modulate nociceptive transmission. Brain Res **397** : 37-46, 1986.
9) Behbehani MM, Jiang MR, Chandler SD, et al : The effect of GABA and its antagonists on midbrain periaqueductal gray neurons in the rat. Pain **40** : 195-204, 1990.
10) Clements JR, Beitz AJ, Fletcher TF, et al : Immunocytochemical localization of serotonin in the rat periaqueductal gray - a quantitative light and electron-microscopic study. J Comp Neurol **236** : 60-70, 1985.
11) Schul R and Frenk H : The role of serotonin in analgesia elicited by morphine in the periaqueductal gray-matter (pag). Brain Res **553** : 353-357, 1991.
12) de Luca M CZ, Brandao ML, Motta VA, et al : Antinociception induced by stimulation of ventrolateral periaqueductal gray at the freezing threshold is regulated by opioid and 5-HT2A receptors as assessed by the tail-flick and formalin tests. Pharmacology Biochemistry and Behavior **75** : 459-466, 2003.
13) Albin RL, Makowiec RL, Hollingsworth Z, et al : Excitatory amino-acid binding-sites in the periaqueductal gray of the rat. Neurosci Lett **118** : 112-115, 1990.
14) Tolle TR, Berthele A, Zieglgansberger W, et al : The differential expression of 16 nmda and non-nmda receptor subunits in the rat spinal-cord and in periaqueductal gray. J Neurosci **13** : 5009-5028, 1993.
15) Mao JR : NMDA and opioid receptors : Their interactions in antinociception, tolerance and neuroplasticity. Brain Res Rev **30** : 289-304, 1999.
16) Jacquet YF : The nmda receptor-central role in pain inhibition in rat periaqueductal gray. Eur J Pharmacol **154** : 271-276, 1998.
17) Berrino L, Oliva P, Rossi F, et al : Interaction between metabotropic and NMDA glutamate receptors in the periaqueductal grey pain modulatory system. Naunyn-Schmiedeberg's Arch Pharmacol **364** : 437-443, 2001.
18) Miguel TT and Nunes-de-Souza RL : Defensive-like behaviors and antinociception induced by NMDA in-

jection into the periaqueductal gray of mice depend on nitric oxide synthesis. Brain Res **1076** : 42-8, 2006.
19) Chiou LC and Chou HH : Characterization of synaptic transmission in the ventrolateral periaqueductal gray of rat brain slices. Neuroscience **100** : 829-834, 2000.
20) Zimmermann M : Ethical guidelines for investigations of experimental pain in conscious animals. Pain **16** : 109-110, 1983.
21) Seltzer Z, Dubner R, Shir Y : A novel behavioral-model of neuropathic pain disorders produced in rats by partial sciatic-nerve injury. Pain **43** : 205-218, 1990.
22) Ye JH, Zhang JL, Xiao C, et al : Patch-clamp studies in the CNS illustrate a simple new method for obtaining viable neurons in rat brain slices : Glycerol replacement of NaCl protects CNS neurons. J Neurosci Methods **158** : 251-259, 2006.
23) Tsuchiya M, Yamazaki H, Hori, Y : Enkephalinergic neurons express 5-HT3 receptors in the spinal cord dorsal horn : Single cell RT-PCR analysis. Neuroreport **10** : 2749-2753, 1999.
24) Fukushima T, Tomitori H, Iwata H, et al : Differential expression of NMDA receptor subunits between neurons containing and not containing enkephalin in the mouse embryo spinal cord. Neurosci Lett **391** : 11-16, 2005.
25) Bernard JF, Dallel R, Raboisson P, et al : Organization of the efferent projections from the spinal cervical enlargement to the parabrachial area and periaqueductal gray : A PHA-L study in the rat. J Comp Neurol **353** : 480-505, 1995.
26) Keay KA, Feil K, Gordon BD, et al : Spinal afferents to functionally distinct periaqueductal gray columns in the rat : An anterograde and retrograde tracing study. J Comp Neurol **385** : 207-229, 1997.
27) Fields HL and Basbaum AI : Central nervous system mechanisms of pain modulation. In : Wall, P.D., Melzack R. (Eds.), Textbook of pain. Churchill Livingstone, London, pp : 309-329, 1999.
28) Millan MJ : Descending control of pain. Prog Neurobiol **66** : 355-474, 2002.
29) Hollmann M and Heinemann S : Cloned glutamate receptors. Annu Rev Neurosci **17** : 31-108, 1994.
30) Mori H and Mishina M : Structure and function of the nmda receptor-channel. Neuropharmacology **34** : 1219-1237, 1995.
31) Monyer H, Burnashev N, Laurie DJ, et al : Developmental and regional expression in the rat-brain and functional-properties of 4 nmda receptors. Neuron **12** : 529-540, 1994.
32) Takahashi T, Feldmeyer D, Suzuki N, et al : Functional correlation of NMDA receptor epsilon subunits expression with the properties of single-channel and synaptic currents in the developing cerebellum. J Neurosci **16** : 4376-4382, 1996.
33) Flint AC, Maisch US, Weishaupt JH, et al : NR2A subunit expression shortens NMDA receptor synaptic currents in developing neocortex. J Neurosci **17** : 2469-2476, 1997.
34) Isaev D, Gerber G, Park SK, et al : Facilitation of NMDA-induced currents and Ca2+ transients in the rat substantia gelatinosa neurons after ligation of L5-L6 spinal nerves. Neuroreport **11** : 4055-4061, 2000.
35) Karlsson U, Sjodin J, Moller KA, et al : Glutamate-induced currents reveal three functionally distinct NMDA receptor populations in rat dorsal horn-effects of peripheral nerve lesion and inflammation. Neuroscience **112** : 861-868, 2002.
36) Iwata H, Takasusuki T, Yamaguchi S, et al : NMDA receptor 2B subunit-mediated synaptic transmission in the superficial dorsal horn of peripheral nerve-injured neuropathic mice. Brain Res **1135** : 92-101, 2007.
37) Delander GE, Schott E, Brodin E, et al : Temporal changes in spinal cord expression of mRNA for substance P, dynorphin and enkephalin in a model of chronic pain. Acta Physiol Scand **161** : 509-516, 1997.
38) Abraham KE, Brewer KL, McGinty JF : Opioid peptide messenger RNA expression is increased at spinal and supraspinal levels following excitotoxic spinal cord injury. Neuroscience **99** : 189-197, 2000.
39) Beitz AJ : The sites of origin brain stem neurotensin and serotonin projections to the rodent nucleus raphe magnus. J Neurosci **2** : 829-842, 1982.
40) Reichling DB and Basbaum AI : Contribution of brainstem GABAergic circuitry to descending antinociceptive controls : II. electron microscopic immunocytochemical evidence of GABAergic control over the projection from the periaqueductal gray to the nucleus raphe magnus in the rat. J Comp Neurol **302** : 378-393, 1990.
41) Lovick TA : Involvement of GABA in medullary

raphe-evoked modulation of neuronal activity in the periaqueductal grey matter in the rat. Experimental Brain Research **137** : 214-218, 2001.

42) Porreca F, Ossipov MH, Gebhart GF : Chronic pain and medullary descending facilitation. Trends Neurosci **25** : 319-325.2002.

43) Vanegas H and Schaible HG : Descending control of persistent pain : Inhibitory or facilitatory? Brain Res Rev **46** : 295-309, 2004.

44) Bago M and Dean C : Sympathoinhibition from ventrolateral periaqueductal gray mediated by 5-HT1A receptors in the RVLM. Am J Physiol-Regul Integr and Comp Physio **280** : R976-R984, 2001.

45) Madden CJ, Ito S, Rinaman L, et al : Lesions of the C1 catecholaminergic neurons of the ventrolateral medulla in rats using anti-D beta H-saporin. Am J Physiol-Regul Integr Comp Physiol **277** : R1063-R1075, 1999.